PHYSICAL REVIEW B VOLUME 8, NUMBER 8 15 OCTOBER 1973

New Electronic Interactions in Rare-Earth Metals at High Pressure*

W. H. Gust and E. B. Royce
Lawrence Livermore Laboratory, University of California, Livermore, California 94550
(Received 2 May 1973)

Equation-of-state data have been obtained from shock-wave experiments on Sc, Y, La, Ce, Pr, Nd, Sm, Eu, Gd, Dy, Yb, and Hf. It is deduced that only Ce exhibits phenomena that may be related to a $4f \rightarrow 5d$ electronic phase transition. An abrupt decrease in compressibility at at high pressure is taken to be evidence of the onset of interaction between closed electron shells in metals. This work is the first identification of the closed-shell electronic interactions in metals in a high-pressure experiment.

INTRODUCTION

It is commonly known that the rare earths form a series of metals with essentially identical chemical properties. Electrons added to these atoms as the atomic number is increased normally go into the $4f$ shells, which are interior to the atoms, and thus do not change the bulk properties of the metals.[1] However, this behavior might be modified as the atoms are brought closer together at high pressure, hence the rare-earth metals form an interesting series of materials for study under shock-wave compression. In addition, one may hope that improved understanding of the equations of state of the lanthanides will provide information that can be applied to the actinide elements. The lanthanide and actinide rare earths together constitute 27% of the Periodic Table yet, prior to this study, shock-wave studies of only thorium and uranium have appeared.[2,3] While this work was in progress,[4] shock-wave-compression data on the rare-earth metals La, Ce, Sm, Dy, and Er were reported by Al'tshuler *et al.*[5]

Most rare-earth metals have the same trivalent electronic structure, i.e., the outer bonding electrons are described by the configuration $5d^1 6s^2$ for all elements except europium and ytterbium. The latter have only two bonding electrons, predominantly in the configuration $6s^2$. In addition to trivalency, cerium and praseodymium exhibit partial tetravalency[1,6] at high pressure or low temperature (i.e., ~100 °K). The similarity in the valence-shell structure is a reflection of the addition of electrons to the deeper-lying $4f$ shell rather than to the $5d$ shell as the atomic number is increased.

In the normal state, each step of increasing atomic number results in higher effective nuclear charge which contracts both the $4f$ and valence-electron shells, thus producing a slight regular reduction of the mean metallic radius from element to element (again excepting europium and ytterbium). The reduction in diameter of the valence-electron shell is a consequence of its interaction with the increased nuclear charge, since the latter is incompletely shielded by the corresponding charge added to the $4f$ shell. This behavior means that these metals allow the study of effects at high pressure caused by small regular variations in interatomic distance or atomic radius. They also allow the study of the effect of varying the relative radii of different electronic shells, since the xenon core ($5p^6$) and $4f$ shell contract more rapidly than do the $5d$ and $6s$ shells as the atomic number is increased.

In the last few years, several static high-pressure measurements of electrical resistance versus compression have been carried out by Bridgman,[6] Drickamer,[7] and Stromberg and Stephens.[8] Recent advances in rare-earth-metal production and refining have made available quantities of materials pure enough to permit meaningful dynamic high-pressure equation-of-state measurements. These, of course, may be compared with the static work.

X-ray diffraction results from experiments in which Gd was quenched at about 40 kbar[9,10] disclosed a retained transition from the hexagonal close-packed (hcp) structure to the Sm-type rhombohedral structure. Further, transitions from the Sm type to the double hexagonal close packed (dhcp) and from the dhcp structure to the face-centered cubic (fcc) structure under pressure have been reported for La, Pr, and Nd.[11] Based upon these results, Jayaraman[12] has proposed that pressure-induced polymorphic transitions in trivalent rare-earth elements occur in the order hcp → Sm type → dhcp → fcc. Similar confirming experiments by McWhan and Stevens[13] have been reported which indicate that Gd, Tb, Dy, and Ho have pressure-induced structure transitions from hcp to the Sm type.

Room-temperature crystal structures associated with the lanthanides and other related elements studied here and the static pressure at which transitions or anomalies have been reported are given in Table I.

If Jayaraman's hypothesis is correct, additional high-pressure phase transitions may be expected for most of these materials. It should be noted,

TABLE I. Crystal structures of the rare-earth metals.

Element	Structure $P=1$ bar	Transition pressure kbar	High-pressure structure	References
Sc	hcp			
Y	hcp			
La	dhcp	23	fcc	11
Ce	fcc	8–15	fcc	6, 11
		50	fcc	14
		···	hcp	15
Pr	dhcp	40	fcc	11
Nd	dhcp	50	fcc	11
Sm	Sm type (rhombic)	···	dhcp	10
Eu[a]	bcc	150	···	7
Gd	hcp	20–25	Sm type	6, 9, 13
Dy	hcp	50	Sm type	8, 13
Yb[a]	fcc	40	bcc	16, 17, 18
Hf	hcp			

[a]Divalent metals.

however, that these particular types of transformations exhibit very small volume changes, of the order of 1%, and will probably not be resolved in measurements made with shock-wave techniques. Also, Stephens[17] and McWhan *et al.*[18] report the 40-kbar transition obtained statically in Yb to be a very slow transformation: A rate-dependent transition may not be driven to completion and thus not be apparent in a dynamic experiment.

Cerium undergoes unique transitions from an expanded fcc → dhcp → contracted fcc as temperature is reduced from 298 to about 100 °K. Further, x-ray powder diffraction studies under pressure by Lawson and Tang[19] disclosed that the initial fcc modification, stable at atmospheric pressure, is converted abruptly to a contracted fcc lattice at about 10 kbar. The volume change at the transition is about 10%, but an additional anomalous contraction of about 5% occurs progressively with increasing pressure below the transition. The latter volume change is believed to be one of the results of a redistribution of electrons from the $4f$ to the $5d$ band, thereby forming a stronger metallic bond which, in turn, increases the density of the material. The high-pressure modification exhibited tetravalent characteristics. Recently Wittig[20] discovered that Ce transforms to a superconductor at 50 kbar and 1.3 °K. X-ray diffractometry by Franceschi and Olcese[14] disclosed a tetravalent strongly collapsed fcc structure (4.4% volume change), but similar measurements by McWhan[15] indicated a slightly distorted hcp structure.

From the discussion above, it appeared that there would be interest in determining the high-pressure dynamic equation of state of Ce and in observing whether or not neighboring lanthanides exhibit similar behavior at high pressures. Drickamer[7] and others have reported irregularities in the change in electrical resistance as a function of static pressure for almost all the rare earths. This offers an opportunity to correlate discontinuities found in dynamic high-pressure equation-of-state measurements with previously reported anomalies. This paper reports on dynamic determinations of Hugoniot parameters from about 0.1 to 1 Mbar and the interpretation of the data with respect to the previously mentioned qualities for the rare-earth elements, cerium (58), praseodymium (59), neodymium (60), samarium (62), europium (63), gadolinium (64), dysprosium (66), and ytterbium (70). The group-III B homologues scandium (21), yttrium (39), and lanthanum (57), which have properties similar to those of the rare earths, and the group-IV B element hafnium (72) which follows the series were also studied.

PROCEDURE

Application of the well-known Hugoniot relations[21–23] used in this work requires a determination of shock and particle velocities. In the work reported here, shock and free-surface velocities were measured by the flash-gap technique.[21,22,24,25] Briefly this consists of placing sample discs on a base plate of a known equation of state, for example, 2024 Al or copper alloy 356, and then exposing the materials to planar shock generated by high explosives. Shock and free-surface transit times are obtained from streak photographs of intense flashes of light which occur when the free or unrestrained surfaces of the shocked material close small appropriately located argon- or xenon-filled gaps. Particle velocity was determined by the impedance-matching technique.[21–23] Low-pressure phase transitions made the free-surface-velocity measurements inaccurate. Hence the free-surface approximation, $U_p \cong \frac{1}{2} U_{fs}$ was used merely to monitor the validity of the impedance match.

When the shock velocity–versus–particle-velocity plot is linear, i.e., $U_s = C + SU_p$, as was the case for all materials measured here, the Hugoniot relations for pressure and volume may be expressed as

$$P = \rho_0 U_p (C + SU_p) \ , \tag{1}$$

$$V/V_0 = [C + (S-1)U_p]/C + SU_p \ , \tag{2}$$

$$P = \rho_0 C^2 \eta / (1 - S\eta)^2 \ , \tag{3}$$

where

$$\eta = 1 - \frac{V}{V_0} \quad \text{and} \quad V/V_0 = \rho_0/\rho \ .$$

Fits to the experimental data [Eqs. (1)–(3)] and the Mie-Grüneisen equation of state

$$P - P_K = (\gamma/V)(E - E_K) \tag{4}$$

were combined to yield Hugoniots and 0 °K isotherms.[22,24,26] For these fits Grüneisen γ's were obtained from

$$\gamma(V) = -\left(\tfrac{2}{3} - \tfrac{1}{3}t\right) - \frac{V}{2}\frac{\partial^2(P_K V^{2t/3})}{\partial V^2}\Big/\frac{\partial(P_K V^{2t/3})}{\partial V}\ , \tag{5}$$

where $t = 1$ produces the Dugdale-McDonald γ that was used in this work. Temperatures were calculated with standard techniques.[24]

High-explosive shock-generating systems were used to produce planar shock waves at pressure levels which ranged from about 80 to 800 kbar in Al. These systems were designed so as to eliminate edge rarefactions from the regions where measurements were made. In order to preserve material purity, sample densities were determined by immersion in Dow-Corning diffusion pump oil and the samples were transported and assembled in an argon atmosphere. In each experiment a slight overpressure of xenon was maintained after removal from the dry box.

Total impurities from spectrographic analyses made by the supplier are shown in Table II. The major impurities noted were other rare-earth metals, calcium and silicon. A chemical analysis was made on the most reactive element, La. It revealed that less than 0.3-at.% H_2, O_2, and N_2 combined was present. Variations in densities from sample to sample of like material were usually less than 0.5% but for Eu, which is also quite reactive, it was about 1.1%. Density variations for the materials are listed in the results.

Sonic velocities were measured for each material.[27] The measurements were stated to be accurate within about 1% for a given sample but the determinations varied as much as 3% from sample to sample. The average results were used to compute the moduli listed in Table III. Figure 1 con-

TABLE II. Impurities in the rare-earth samples.

Sample	Other rare earths (at.%)	Other elements[a] (at.%)	Total impurities (at.%)
Sc	0.003	0.054	0.057
Y	0.05	0.292 (0.25 Ta)	0.35
La	0.091	0.034	0.125
Ce	0.075	0.035	0.110
Pr	0.04	0.087 (0.05 Si)	0.127
Nd	0.075	0.021	0.096
Sm	0.033	0.17 (0.1 Si)	0.203
Eu	0.016	0.097	0.113
Gd	0.07	0.034	0.104
Dy	0.065	0.034	0.099
Yb	0.008	0.115 (0.1 Ca)	0.123
Hf	...	0.06 plus 3 to 4.5 Zr	3.1–4.6

[a]Ca, Si, Mg, C, Fe, and Cu.

TABLE III. Elastic constants from ultrasonic measurements.

Quantity	Unit	Sc	Y	La	Ce	Pr	Nd	Sm	Eu	Gd	Dy	Yb	Hf
Density	g/cm^3	3.01	4.51	6.13	6.78	6.76	7.0	7.48	5.32	7.91	8.56	7.0	12.8
Longitudinal velocity, C_L	mm/μsec	5.69	4.24	2.77	2.35	2.72	2.82	2.92	2.26	2.94	2.96	1.88	3.87
Shear velocity, C_s	mm/μsec	3.25	2.28	1.53	1.32	1.49	1.55	1.63	1.19	1.68	1.72	1.02	2.08
Adiabatic bulk velocity, [a] C_B	mm/μsec	4.28	3.32	2.13	1.79	2.11	2.18	2.23	1.79	2.21	2.19	1.46	3.03
Young's modulus, E	10^{11} dyn/cm^2	7.99	6.09	3.66	3.0	3.85	4.31	5.06	1.96	5.61	6.30	1.88	14.4
Shear modulus, G	10^{11} dyn/cm^2	3.18	2.35	1.43	1.18	1.50	1.68	1.99	0.75	2.23	2.53	0.73	5.56
Poisson's ratio		0.257	0.296	0.280	0.269	0.283	0.283	0.272	0.308	0.257	0.245	0.290	0.296
Adiabatic compressibility, β	10^{-12} cm^2/dyn	1.81	2.01	3.57	4.60	3.34	3.02	2.68	5.86	2.60	2.43	6.68	0.85
Grüneisen constant, [b] γ		1.19	1.39	0.37	0.35	0.45	0.64	0.39	1.50	0.63	0.99	1.28	1.27

[a]$C_B^2 = C_L^2 - \frac{4}{3}C_s^2$.

[b]$\gamma = 3\alpha V/(\beta C_P - 9\alpha^2 TV)$; values for α and C_P from Ref. 1.

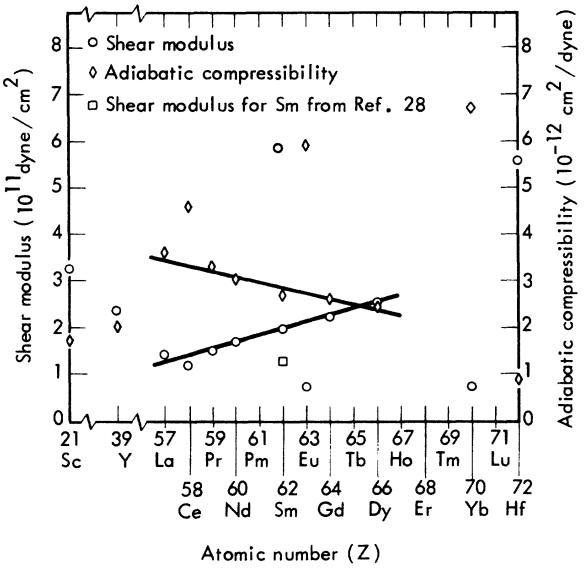

FIG. 1. Data confirming the linear trend of shear modulus and adiabatic compressibility versus atomic number noted by Smith *et al.* (Ref. 28).

firms the linear trend of the shear modulus and compressibility versus atomic number that was noted by Smith *et al.*[28] Except for Sm the data were in agreement. For Sm, the value of the shear modulus obtained here fits the linear trend much better, indicating that the deviation of Sm in their data may have been caused, not by some complex modification of crystal structure, but by material impurities. The divalent elements Eu and Yb do not fit the trend.

RESULTS

The Hugoniot parameters measured are listed in Table IV. Plots of shock velocity versus particle velocity and pressure versus volume follow. The inserted figures give resistance-versus-pressure curves based on the work of Bridgman[29] and Drickamer.[7] Coefficients for the straight-line relations found in (U_s, U_p) plots are recorded in Table V.

Figure 2 presents Hugoniot parameters for scandium. The single straight line obtained does not extrapolate to the C_B measured in this work but agrees better with the value obtained by Brown *et al.*[30] with material of higher purity. The magnitude of C_B is about twice that of most of the lanthanides indicating a much less compressible initial state. The electronic structure outside the full argon shell ($3p^6$) is $3d^1 4s^2$ with a metallic radius of 1.641 Å at normal temperature and pressure. The slope $dU_s/dU_p = 0.85$ is about the same as the initial slopes for several of the lanthanides and is in fair agreement with the initial slope of Al'tshuler's data.[31] Their data indicate a kink in the (U_s, U_p) plot at 1.23 Mbar, a pressure greater than that was attained here.

In Fig. 3 the (U_s, U_p) plot for yttrium is similar to those obtained for most of the rare earths. The initial segment intercepts at C_B indicating that no large volume phase transition has occured in the low-pressure region. For yttrium the electronic structure outside the krypton ($4p^6$) shell is $4d^1 5s^2$ with a metallic radius of 1.801 Å. This is about the same as the radii of the lanthanides. Bridgman's relative-resistance data[29] indicate an almost linear decrease from 1.0 to 0.9 between 0 and 70 kbar; relative-resistance data at higher pressure are not available. The pressure corresponding to the kink, marked on the (P, V) diagram, was about 280 kbar and the temperature was about 1050 °K.

The results obtained for lanthanum, Fig. 4, are in excellent agreement with the data of Al'tshuler, *et al.*[31] The initial slope intercepts at C_B. The only anomaly noted was the slope discontinuity at velocity values corresponding to a pressure of about 250 kbar and a temperature of 1590 °K. Bridgman's data[29] indicate a cusp in the electrical resistance measurements at 25 kbar and a 0.28% volume change at 23 kbar with no further discontinuities to 100 kbar. Piermarini and Weir[11] reported a dchp → fcc transformation at an unmeasured pressure presumed to be about 23 kbar. None of these phenomena are discernible in these dynamic measurements.

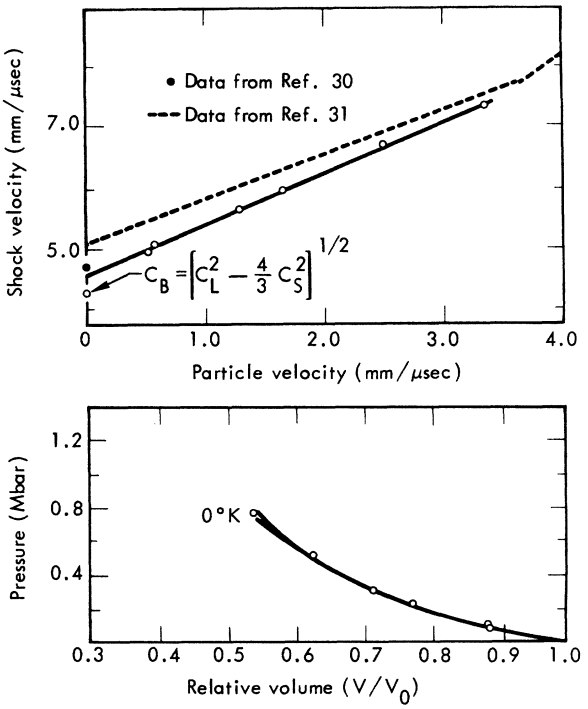

FIG. 2. Scandium Hugoniot parameters. C_B is about twice that of most lanthanides. The slope, $dU_s/dU_p = 0.85$, is in fair agreement with Ref. 31.

TABLE IV. Summary of experimental data.

Element and atomic no. (Z)	Average initial density (g/cc)	Density variation (rms) (%)	Shock velocity (U_s) (mm/μsec)	Particle velocity (U_p) (mm/μsec)	Free surface velocity (mm/μsec)	Pressure (P) (kbar)	Relative volume (V/V_0)	Temperature on Hugoniot (10^3 °K)
Sc	3.012	0.32	4.95	0.53	0.97	79	0.893	0.33
(21)			5.07	0.58	0.96	89	0.886	0.34
			5.66	1.29	2.49	219	0.771	0.56
			5.96	1.68	3.09	301	0.718	0.81
			6.71	2.50	5.06	505	0.628	1.71
			7.37	3.36	6.67	746	0.543	3.55
Y	4.513	0.35	3.67	0.56	0.97	93	0.847	0.35
(39)			3.97	0.96	1.63	172	0.758	0.51
			4.15	1.16	2.00	217	0.721	0.66
			4.19	1.24	2.12	234	0.704	0.76
			4.49	1.62	3.03	329	0.638	1.4
			4.88	1.92	3.77	423	0.607	2.05
			5.29	2.35	4.72	562	0.555	4.03
			6.27	3.15	6.20	891	0.497	8.7
La	6.134	0.46	2.61	0.53	0.97	85	0.798	0.51
(57)			3.37	1.12	2.27	225	0.667	1.59
			3.85	1.53	2.98	361	0.602	3.35
			4.90	2.17	4.45	653	0.556	6.5
			5.61	2.70	•••	929	0.520	11.9
			5.93	3.0	6.09	1090	0.505	15.5
Ce	6.759	0.65	1.90	0.58	1.12	74	0.696	1.26
(58)			2.69	0.90	1.66	164	0.666	1.79
			3.14	1.10	2.17	233	0.649	2.15
			4.06	1.69	3.62	469	0.583	5.40
			4.78	2.08	4.26	674	0.565	7.05
			5.48	2.62	5.32	969	0.522	14.5
			5.93	2.93	6.01	1170	0.506	•••
Pr	6.758	0.22	2.55	0.52	0.97	89	0.795	0.4
(59)			3.02	1.15	2.11	232	0.618	1.39
			3.53	1.59	3.02	374	0.549	3.3
			4.43	2.11	4.30	621	0.525	5.56
			5.03	2.53	5.03	849	0.497	11.5
			5.69	3.01	6.38	1140	0.472	•••
Nd	6.983	0.49	2.50	0.49	0.82	86	0.802	0.41
(60)			2.50	0.50	1.00	88	0.798	0.41
			2.76	0.72	1.58	139	0.737	0.59
			2.84	0.83	1.67	165	0.706	0.75
			3.12	1.11	2.21	241	0.643	1.37
			3.53	1.48	2.93	365	0.579	2.94
			4.33	2.02	4.31	613	0.533	5.5
			5.38	2.85	5.90	1070	0.469	14.6
Sm	7.477	0.07	2.73	0.49	0.94	101	0.818	0.41
(62)			3.15	1.08	2.11	255	0.655	1.25
			3.62	1.53	2.93	414	0.577	2.88
			4.29	2.03	4.23	653	0.525	5.55
			4.82	2.47	5.10	890	0.488	9.4
			5.37	2.96	6.11	1190	0.448	16.8
Eu	5.282	1.1	2.03	0.63	1.00	67	0.691	0.52
(63)			2.06	0.59	1.01	65	0.711	0.47
			2.39	0.97	•••	122	0.596	0.96
			2.69	1.30	2.69	185	0.515	1.85
			3.07	1.70	3.30	276	0.446	4.03
			3.33	2.07	4.15	363	0.378	22.5
			3.85	2.21	4.38	450	0.426	5.2

TABLE IV. (*Continued*).

Element and atomic no. (Z)	Average initial density (g/cc)	Density variation (rms) (%)	Particle velocity (U_s) (mm/μsec)	Particle velocity (U_p) (mm/μsec)	Free surface velocity (mm/μsec)	Pressure (P) (kbar)	Relative volume (V/V_0)	Temperature on Hugoniot (10^3 °K)
			4.54	2.79	5.76	669	0.385	19.0
			5.13	3.26	6.57	883	0.365	•••
Gd (64)	7.912	0.24	2.66	0.47	0.92	99	0.821	0.41
			2.85	0.67	1.48	152	0.764	0.55
			3.14	1.05	2.06	262	0.665	1.25
			3.59	1.42	2.82	403	0.605	2.43
			4.31	1.93	3.98	660	0.551	4.79
			5.26	2.76	5.69	1150	0.476	13.3
Dy (66)	8.559	0.02	2.57	0.41	0.85	91	0.839	0.39
			3.13	0.98	2.05	262	0.686	1.03
			3.45	1.32	2.70	391	0.615	1.97
			4.09	1.94	3.91	682	0.524	4.95
			5.08	2.76	5.66	1200	0.456	12.2
Yb (70)	6.966	0.75	1.85	0.47	1.02	61	0.744	0.35
			2.14	0.84	1.59	125	0.607	0.75
			2.20	1.06	2.12	163	0.516	2.35
			2.29	0.94	1.77	150	0.589	0.89
			2.41	1.17	2.07	197	0.515	2.35
			2.57	1.19	2.39	214	0.535	1.71
			2.64	1.29	2.94	270	0.511	2.28
			2.93	1.50	3.04	306	0.489	3.88
			3.90	2.18	4.40	593	0.441	11.2
			4.89	2.99	5.98	1020	0.389	•••
Hf (72) (+3% Zr)	12.83	0.07	3.36	0.37	0.64	158	0.891	0.35
			3.67	0.70	1.51	331	0.808	0.52
			3.86	0.99	1.91	489	0.744	0.92
			4.25	1.35	2.91	738	0.682	1.91
			4.77	1.77	3.61	1090	0.628	4.1
			5.51	2.35	4.76	1670	0.573	9.04

The (U_s, U_p) plot for cerium, Fig. 5, shows but a single line, and extrapolation of the single line does not intercept at C_B. This anomaly is undoubtedly related to the known phase transitions at 7 and 50 kbar,[19,20] as well as the cusps found in the pressure-resistance curves at 65 kbar by Bridgman[29] and at 200 kbar by Drickamer.[7] Data scatter in the low-pressure region is probably related to the 15% volume change found for the 7-kbar transition. In Fig. 5, note the abrupt change in

TABLE V. Coefficients for $U_s = C + SU_p$

Element	Density (g/cm^3)	Bulk sound speed $C_B = (C_L^2 - \frac{4}{3}C_S^2)^{1/2}$	Intercept (C_1) (mm/μsec)	Slope (S_1)	Intercept (C_2) (mm/μsec)	Slope (S_2)
Sc (21)	3.012	4.28 4.67[a]	4.56	0.85	•••	•••
Y (39)	4.513	3.32	3.30	0.71	2.69	1.12
La (57)	6.134	2.13	2.08	1.12	1.71	1.43
Ce (58)	6.780	1.79	•••	•••	1.34[b]	1.59
Pr (59)	6.758	2.11	2.09	0.83	1.15	1.53
Nd (60)	7.001	2.18	2.03	0.98	1.60	1.32
Sm (62)	7.477	2.23	2.23	0.88	1.77	1.22
Eu (63)	5.305	1.79	1.51	0.89	1.13	1.22
Gd (64)	7.912	2.21	2.22	0.90	1.86	1.24
Dy (66)	8.559	2.19	2.20	0.95	1.74	1.21
Yb (70)	6.998	1.46	1.49	0.78	1.0	1.31
Hf (72)	12.835	3.03	3.02	0.86	2.56	1.25

[a]Data from Ref. 30.

[b]For $U_p > 1.0$ mm/μsec.

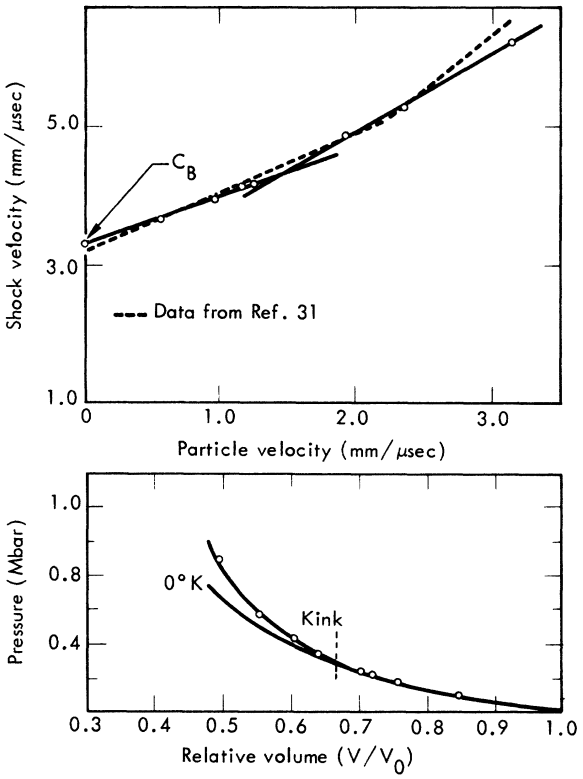

FIG. 3. Yttrium Hugoniot parameters. The kink in the (U_s, U_p) plot, marked on the (P, V) curve, occurred at about 280 kbar and 1050°K.

electrical resistance associated with this transition. Our data seem to indicate that the transition may not have been driven to completion in the low-pressure experiments. Two-wave shock structures are not resolved by the flash-gap technique and hence there is a relatively large error in these particular low-pressure measurements.

No discontinuities are apparent in the shock-particle-velocity plot for Praseodymium, Fig. 6, other than the kink which occurs at (U_s, U_p) values equivalent to about 300 kbar and a temperature of 1330°K. Drickamer's curves[7] show discontinuities at 40 and 200 kbar. Correlation between the dhcp→fcc transition at 40 kbar (Table I) is apparent in the electrical resistance curve but not in the (U_s, U_p) plot. There is qualitative agreement between the broad maximum at about 340 kbar and the pressure corresponding to the (U_s, U_p) kink. Neither the pressure-resistance nor the (U_s, U_p) curves resemble the curves found for cerium. It should be noted that for Pr the resistance increases with applied pressure, opposite the behavior of the other rare earths excepting Eu and Yb. Nevertheless the (U_s, U_p) plot has the typical concave upward kink.

Figure 7 displays the Hugoniot parameters for neodymium. The initial line segment does not intercept at C_B. This anomaly is probably related to the known dchp→fcc transition[11] at about 50 kbar. There is good agreement with the Al'tshuler, *et al.* data.[31] The temperature and pressure which correspond to the (U_s, U_p) kink are 1640°K and 280 kbar. Drickamer's curve[7] shows fairly sharp discontinuities at about 90 and 120 kbar which may be related to the above transition but none at the pressure which corresponds to the kink.

The (U_s, U_p) plot for samarium, Fig. 8, extrapolates to C_B and the kink values correspond to a temperature of 1650°K and a pressure of 310 kbar. There are no discontinuities in the P-vs-R plot which correspond to the kink pressure. Excellent agreement with the Al'tshuler *et al.* data[31] was obtained for the initial slope but their slope for the second segment is steeper than ours.

The discontinuity in the (U_s, U_p) plot for Europium (divalent), Fig. 9, appears to be of a different character than that of the trivalent lanthanides. The intercept at $U_p = 0$ does not coincide with C_B thus indicating a low-pressure transformation. Drickamer's R-vs-P data[7] indicates the resistance increased with pressure and a sharp rise, typical of a first-order transition, occurred at about 150

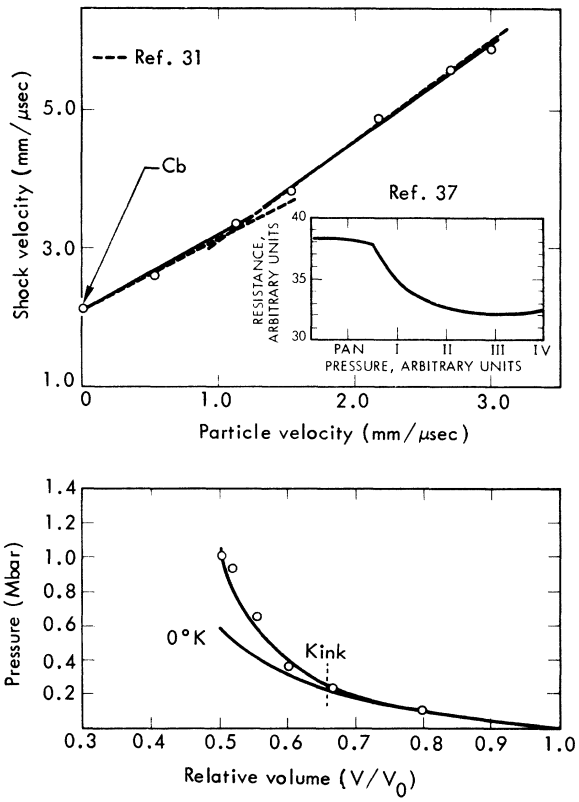

FIG. 4. Lanthanum Hugoniot parameters. The temperature and pressure corresponding to the (U_s, U_p) kink are about 250 kbar and 1590°K. None of the reported phase transformations[11,29] are discernible in these dynamic measurements.

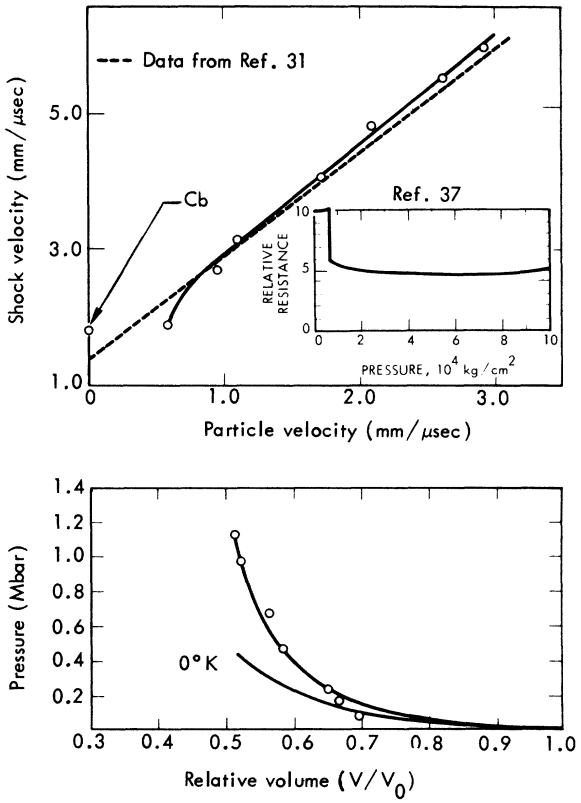

FIG. 5. Cerium Hugoniot parameters. Data scatter in the low-pressure region is probably related to the 15% volume change reported[19,20] for the 7-kbar transition, as is the failure of the single (U_s, U_p) line to intercept at C_B.

kbar followed by a small maximum at about 180 kbar. Although the (U_s, U_p) data for $1.3 < U_p < 2$ mm/μsec appear to be aligned with the initial line segment, the intersection of the extrapolation of the second line segment indicates that a sluggish or time-dependent transformation may have occurred. The temperature and pressure corresponding to the intersection as shown are 1810 °K and 190 kbar which agrees qualitatively with Drickamer's data.[7] On the other hand, if the odd discontinuity at $U_p \approx 2.1$ mm/μsec is correct the corresponding pressure and temperature are 7700 °K and 360 kbar.

The plot for gadolinium, Fig. 10, exhibits the characteristics found for most rare earths. The intercept is at C_B and the kink occurs at velocity values which correspond to 1400 °K and 260 kbar. The hcp → Sm-type transition at 35 kbar[11] is not discernible in either the (U_s, U_p) or (R, P) plot. Agreement with the data of Al'tshuler *et al.*[31] is fair.

Figure 11 presents the Hugoniot parameters for Dysprosium. The plots are nearly the same as those found for gadolinium. The intercept is at C_B; the temperature and pressure corresponding to the kink are 2720 °K and 480 kbar. Agreement with Al'tshuler's data[31] is good. The hcp → Sm-type transition at 75 kbar[8,13] is not discernible in either plot.

The (U_s, U_p) plot for ytterbium (divalent), Fig. 12, is similar to those obtained for the trivalent rare earths; the temperature and pressure corresponding to the kink were 1230 °K and 130 kbar. The (R, P) plot is like that of strontium, a group-IIA element. Soeurs and Jura[32] have reported that Yb becomes a semiconductor under pressure starting at about 20 kbar and then becomes metallic again at 40 kbar. Hall *et al.*[16] and Hall and Merrill[33] reported that the abrupt reduction in resistance was related to a fcc → bcc phase transition with an 11% volume change which also involves the promotion of a $4f$ electron to the $5d$ level. The data marked were obtained from inclined prism experiments[34] which are capable of resolving the multiple-wave structures usually found with shock-induced polymorphic phase transitions. No multiple wave structures were observed. This implies that the transition must be sluggish or time dependent like the results obtained for cerium and europium.

Figure 13 shows the (U_s, U_p) data for hafnium.

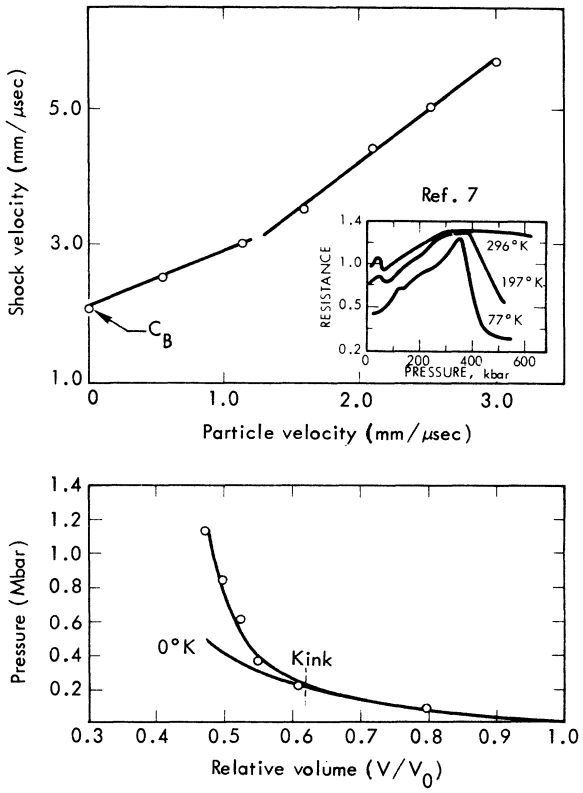

FIG. 6. Praseodymium Hugoniot parameters. The (U_s, U_p) kink occurs at about 300 kbar and 1330 °K, again showing no correlation to known phase transformations and resistance-pressure discontinuities.

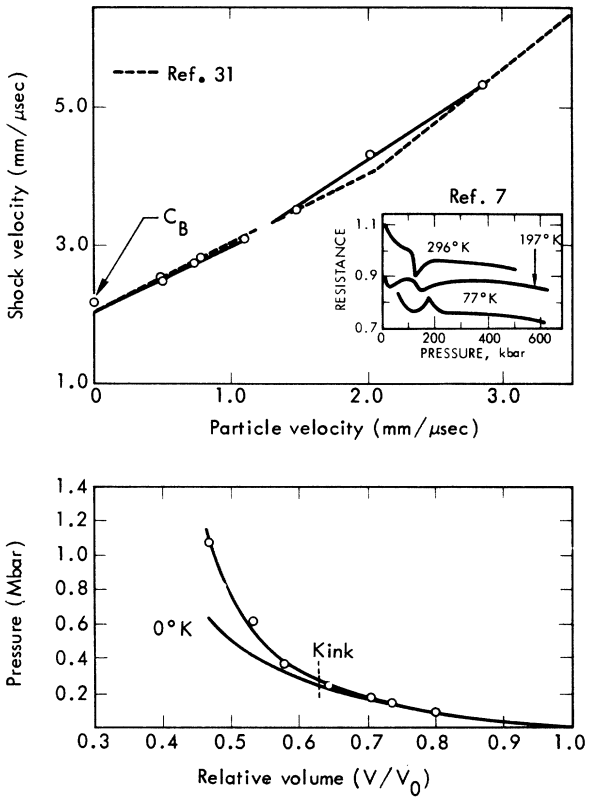

FIG. 7. Neodymium Hugoniot parameters. The temperature and pressure corresponding to the (U_s, U_p) kink are 1640°K and 280 kbar. Neither the known phase transition (Ref. 11) at 50 kbar nor the sharp resistance-pressure discontinuities (Ref. 7) at 90 and 120 kbar appear to correlate with this kink.

This plot is similar to those found for the rare-earth elements. The intercept is at C_B and the kink occurs at velocity values which correspond to 1390°K and 600 kbar. The $(R/R_0, P)$ plot for hafnium[29] decreases linearly from 1.0 to 0.96 in going from 0 to 100 kbar.

DISCUSSION

The plots of U_s vs U_p (Figs. 2–13) were linear for all materials. However, the plots for Y, La, Pr, Nd, Sm, Gd, Dy, and Hf were composed of two line segments which displayed the new and unusual characteristic[35] of being concave upwards. No corresponding discontinuity appears on the pressure-volume plots. (The point where it would appear is indicated on each plot.) The intersection of the two lines marks an abrupt change in the volume derivative of the compressibility and hence is of considerable interest to those concerned with the electronic structure of metals. The primary aim of this discussion is to determine the cause of this discontinuity.

With one exception the plotted initial segment for each of these elements intercepted the y axis near C_B, the ultrasonically measured bulk-sound speed at 1 bar, thus implying that no phase transitions characterized by large volume changes had occurred. For Nd, displacement of the intercept from C_B implies that a shock-induced first-order transition occurs at low pressure. Piermarini and Wier[11] have reported a dhcp → fcc transition for Nd at 50-kbar static pressure.

The (U_s, U_p) plots for the remaining elements, Sc, Ce, Eu, and Yb, display characteristics that are considerably different. Points of interest concerning these are as follows: (a) The slope for Sc, throughout the pressure region measured, is about the same as the initial slopes for the lanthanides. (b) The plot for Ce does not resemble those for its neighbors La and Pr and appears to be unique among the rare-earth metals. (c) Displacement of the intercept from C_B for Eu indicates that a first-order transition occurs at low pressure. (d) The peculiar scatter in the curves for Eu and Yb may be indicative of a very sluggish phase transition accompanied by additional stiffening of the lattice. In the latter case the discontinuity is assumed to be related to a two-wave region,[35,36] a part of a transition that is incompletely driven because of

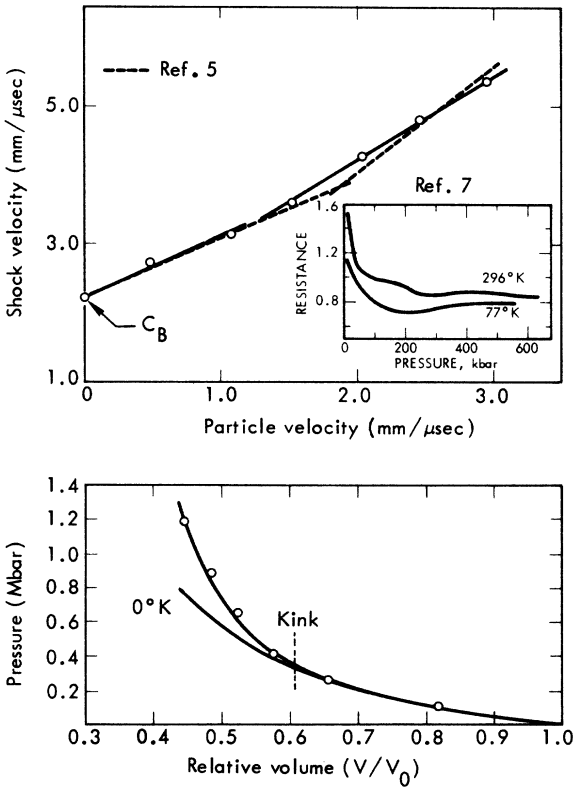

FIG. 8. Samarium Hugoniot parameters. The kink in (U_s, U_p) occurs at 1650°K and 310 kbar. The (R, P) plot contains no corresponding discontinuities.

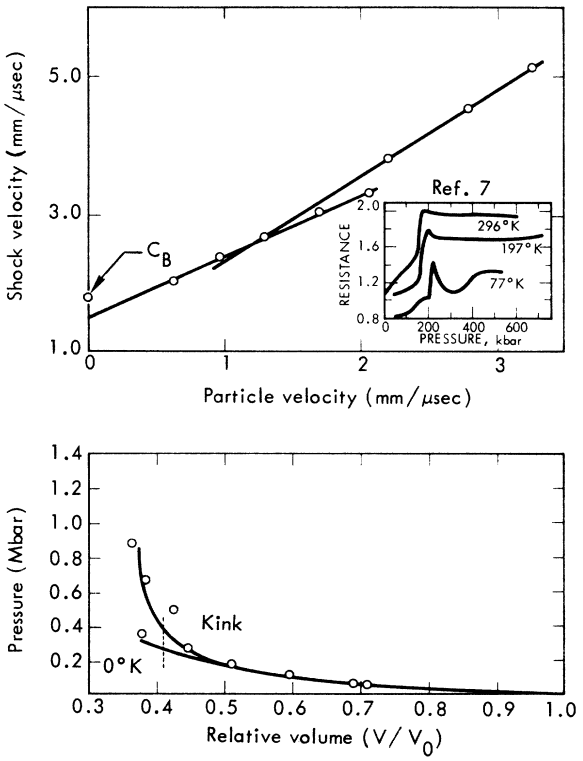

FIG. 9. Europium (divalent) Hugoniot parameters. Note the odd character of the kink. The overlap and the alignment of the points for $1.3 < U_p < 2$ mm/sec suggest a sluggish transformation.

kinetic limitations.

It might be assumed that the (U_s, U_p) kinks are manifestations of melting at high pressure. In applying Simons equation, however, it may be noted that T(kink)/T(melt 1 bar) varies like 0.9 for Gd, 1.2 for Pr, Nd, Sm, and Yb; 1.3 for La; and 1.6 for Dy and Eu. The melting points of the rare-earth metals at $P = 1$ bar increase slowly and regularly with atomic number.[1] The wide range and irregularity of values of the above ratio makes it unlikely that all of the (U_s, U_p) kinks can be caused by melting at high pressure although melting probably has occurred for all except Hf. In other words, one should expect the melting point at high pressure to also increase slowly and regularly with atomic number. The temperatures related to the kinks do not increase slowly and regularly with atomic number. Hence it appears that the (U_s, U_p) kinks are not manifestations of melting at high pressure.

It may be demonstrated[3,22] that, in addition to increasing the initial density of the material, the presence of a significant d-electron population in the conduction band of many metals makes them relatively imcompressible as compared to metals with only s electrons in the conduction band. It may be further shown that the Wigner-Seitz radius of an atom in metals has the same dependence on Z, the atomic number, as does the radius of a particular orbital in the free atom as obtained from Hartree-Fock calculations, as long as the conduction band is less than half-full. For metals with only ns electrons in the conduction band, the radius of the ns orbital must be used, while for metals with $(n-1)d$ ns hybrid conduction bands, the $(n-1)d$ orbital must be used. Figure 14 shows the Wigner-Seitz radii predicted in this way for the rare-earth metals[3,22] (broken lines). Radii of metals with $6s$ conduction bands were normalized to the radii of Cs and Ba, while those with $5d6s$ conduction bands were normalized to Hf, Ta, and W. Also shown is the Z-dependence of the radius of the Xe core ($5p^6$).

The solid curves shown in Fig. 14 represent the experimental Wigner-Seitz atomic radii for the rare earths at several pressures. The data obtained from the 0 °K isotherms calculated from the shock-wave data demonstrate that the regular reduction of atomic radii with Z is not maintained at high pressure.

At zero pressure, most of the rare-earth metals are trivalent, with $5d6s^2$ configuration, and their radii are satisfactorily close to the curve of pre-

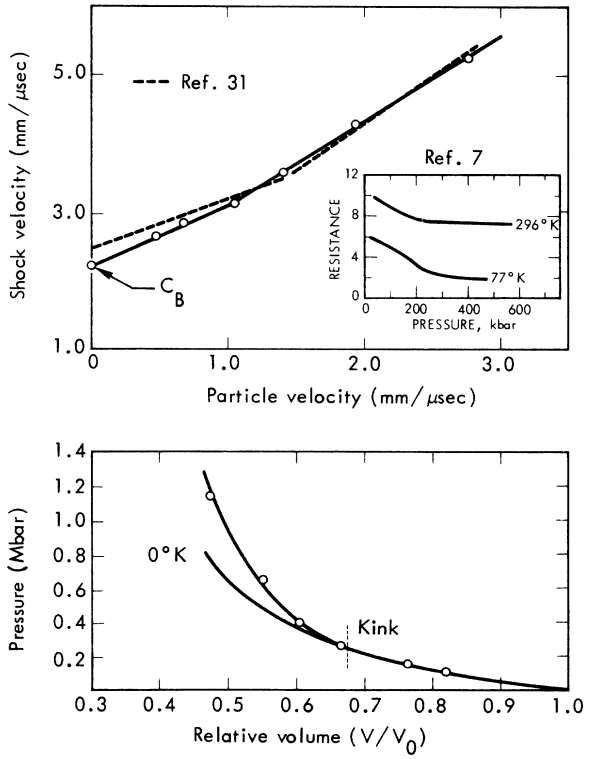

FIG. 10. Gadolinium Hugoniot parameters. The (U_s, U_p) kink comes at 1400 °K and 260 kbar. The phase transition at 35 kbar (Ref. 11) affects neither the (U_s, U_p) nor the (R, P) plot.

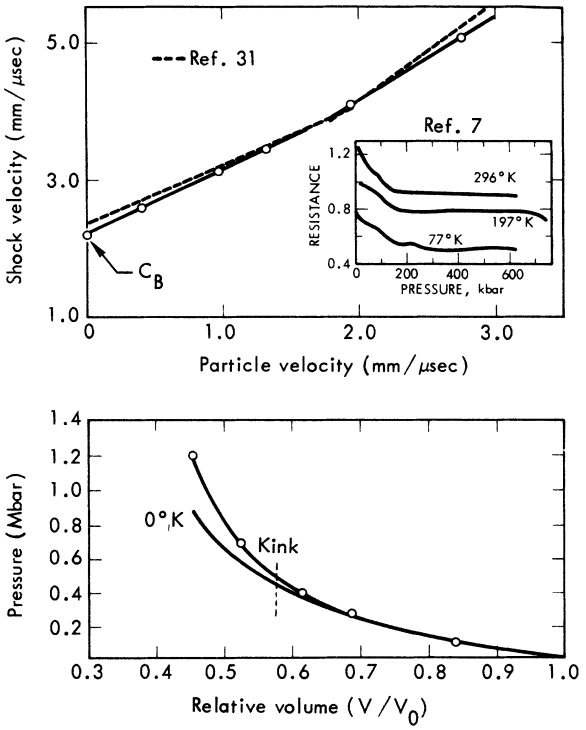

FIG. 11. Dysprosium Hugoniot parameters. Note the similarity to the plots for gadolinium, Fig. 10. The (U_s, U_p) kink occurs at 2720°K and 480 kbar; the known phase transition (Refs. 8 and 13) is undiscernible.

dicted 5*d* radii. Similarly, the divalent metals Eu and Yb, having the $6s^2$ configuration, fall close to the 6*s* curve. Under pressure, however, all of the rare-earth metals appear to be much more compressible than the metals Hf, Ta, or W which have the $5d^n6s^2$ configuration.

Insight into the apparent failure of the trivalent rare-earth metals to exhibit the incompressibility characteristic of metals with *d* electrons in the conduction band may be obtained from Fig. 15. Here the relative change in atomic radius caused by a pressure of 250 kbar is plotted against nitial molar volume for a number of elements which have *d* and *s* electrons in their conduction bands. Sc and Y are aligned with relatively incompressible elements that exhibit *d* character but the rare-earth elements are all plotted near the intersection of the lines which join the 5*d* elements W, Ta, and Hf and the 6*s* elements Ba and Cs.

Since the rare earths are also aligned with the 6*s* elements, it cannot be claimed from arguments based on the Periodic Table that the rare earths should exhibit incompressibility because of the *d* electrons in their conduction band. Rather it appears that the rare earths should exhibit incompressibilities intermediate between those of *d* and *s* character. Thus, arguments[3] that attributed the relative softness to a continuous transfer of electrons from the $5d \rightarrow 4f$ band appear invalid. The earlier conclusions[3] failed to recognize that compressions, as earlier presented, did not properly take into account initial density differences such as between W, Ta, and Hf, on the one hand, and the trivalent rare earths on the other.

According to Lawson,[37] hydrostatic-pressure-induced changes in the electrical resistance of normal metals fall into four, not necessarily independent, categories. These include change in the interaction between the electrons and the lattice waves caused by stiffening of the lattice, the change in the Fermi energy, the appearance of new crystallographic forms, and possible changes in band structures. Ordinary first-order phase transitions and changes in band structure are normally accompanied by resistance discontinuities.

The 4*f* electrons, which are shielded by the 5*p* and 4*d* shells, make no contribution to electrical conductivity. An increase in the number of free electrons per unit volume resulting from a $4f \rightarrow 5d$ transition should cause appreciable variation in conductivity or resistance. This is demonstrated by Bridgman's[29] plot of *P* vs *R* for cerium, inset in Fig. 5. At about 10 kbar of applied pressure the resistance is abruptly reduced to about one-half its initial value. This discontinuity has been related[19] to a 4*f* to 5*d* electronic transition which

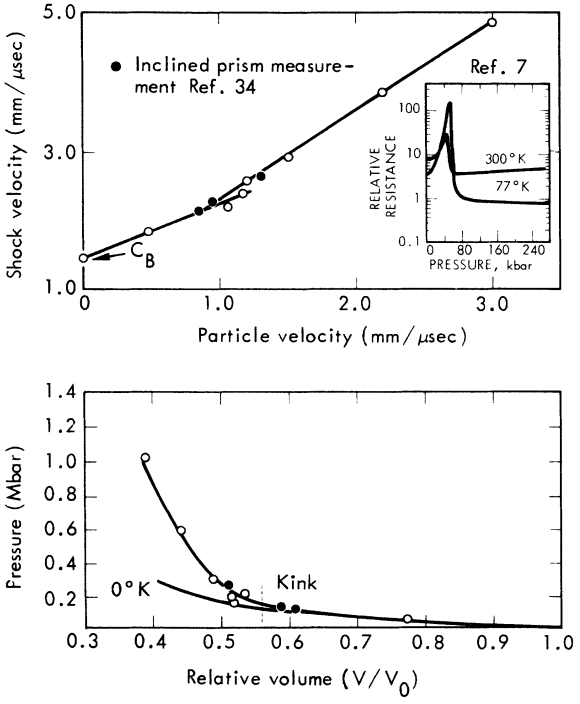

FIG. 12. Ytterbium Hugoniot parameters. The kink in (U_s, U_p) comes at 1230°K and 130 kbar, again showing no correlation with known phase changes.[16,32,33]

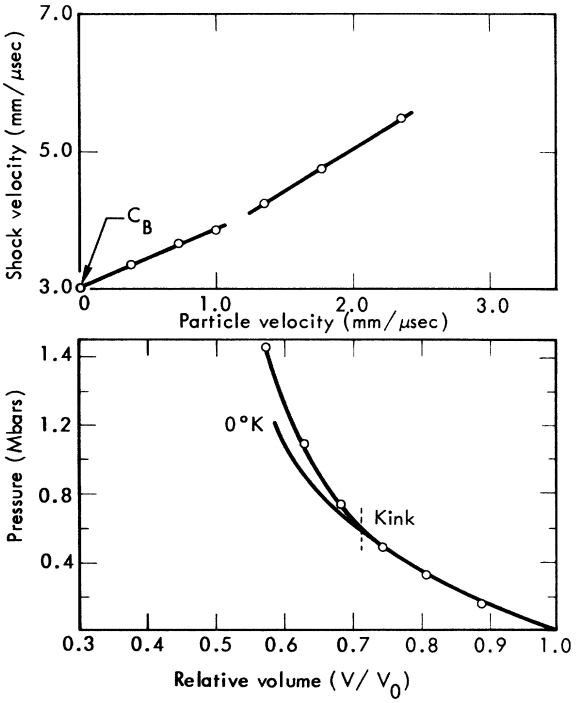

FIG. 13. Hafnium Hugoniot parameters. The kink in velocity values occurs at 1390°K and 600 kbar. No corresponding discontinuity appears in the (R, P) plot.

in turn changes the fcc structure to a contracted fcc structure.

The characteristics of a $6s \rightarrow 5d$ electronic transition have been associated with a transition that occurs in cesium. Here, Fermi[38] suggested that an 11% volume reduction at 50 kbar was caused by the valence electron being forced into an internal or orbit. Jayaraman *et al.*[39] found that the relative electrical resistance of cesium increased markedly but smoothly by a factor of 6, as pressure was increased from 20 to 40 kbar. This response was taken to be a manifestation of a continuous $6s \rightarrow 5d$ electronic transition.

Examination of Drickamer's resistance-versus-pressure curves for the other rare earths[6] shows that none have discontinuities resembling the curves for cerium or cesium, especially for pressures greater than 200 kbar, the pressure regime corresponding to the kinks in the (U_s, U_p) plots. Thus the absence of conductivity discontinuities indicates that the stiffening of rare-earth Hugoniots does not appear to be related to either a $4f \rightarrow 5d$ electronic transition like that of cerium or a $6s \rightarrow 5d$ transition as propose by Al'tshuler *et al.*[5]

Further, at specific volumes where the $4f \rightarrow 5d$ transition in cerium occurs, added population of d band appears energetically favorable.[3] At high compressions, where the Hugoniots stiffen in the other rare earths, no appreciable population of the d band is energetically favorable, as evidenced by the incompressibility of hafnium, tantalum, and tungsten.[3]

Al'tshuler *et al.*[31] and Bakanova and Dudoladov[40] have recently reported shock compression data for Nd, Gd, and Lu and have indicated that a number of elements other than rare earths also exhibit (U_s, U_p) plots that are concave upwards. Their results, obtained at pressures considerably higher than those achieved here, included data for Sc, Cu,

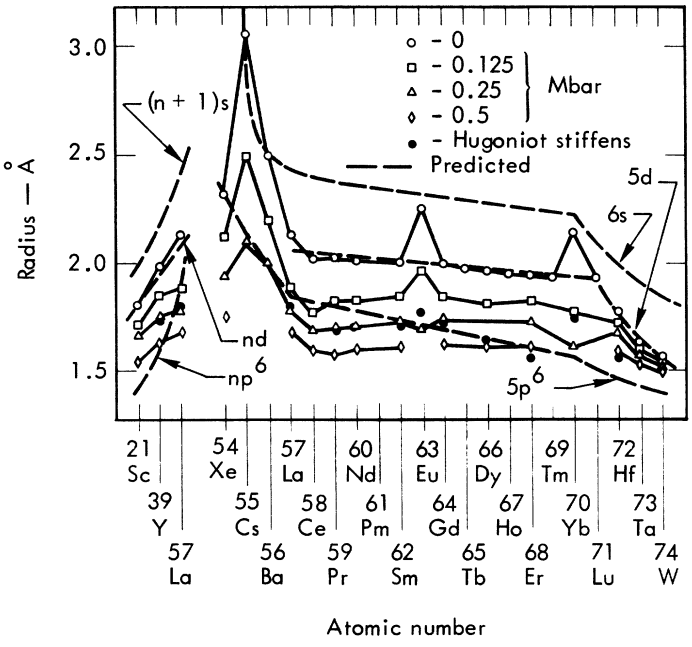

FIG. 14. Wigner-Seitz atomic radii vs atomic number at several pressures, all at 0°K, as calculated from shock-wave measurements. The broken lines are atomic shell radii at $P = 0$ from Ref. 3. The experimental points for Er are calculated from data of Ref. 5, and for Xe, Cs, Ta, and W from data references in Refs. 2 and 3. The solid circles (•) shown mark the points where the various rare-earth Hugoniots stiffen. Note that for La, Pr, Nd, Sm, Dy, Er, and probably Gd, this stiffening occurs only after the material has been compressed to a volume where the Xe cores overlap.

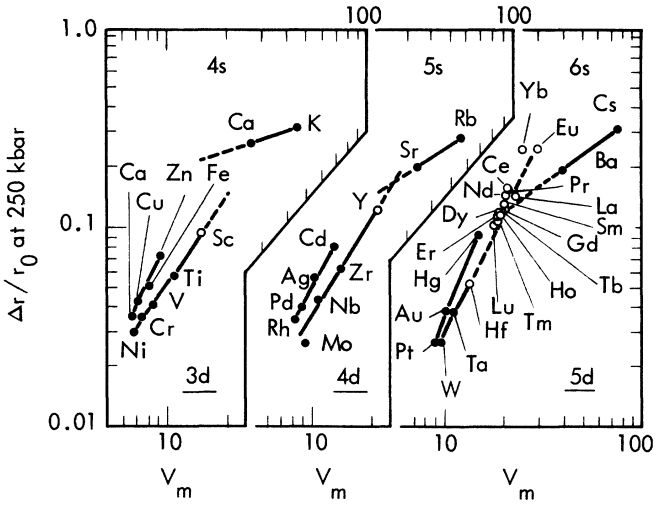

FIG. 15. Relative atomic radii vs molar volume for a number of elements which have *d* and *s* electrons in their conduction bands. Sc, Y, and Hf are aligned with the relatively incompressible elements which have *d* electrons in their conduction bands while the rare earths are grouped about the intersection of lines from elements exhibiting *d* and *s* character.

V, Sr, Y, Zr, and Nb. None of these elements have incomplete shells available to accept a conduction electron in an electronic phase transition. One should therefore expect compressional behavior different than that exhibited by the rare earths. It was argued earlier that a $4f \rightarrow 5d$ transition is not energetically favorable in the rare earths at high compression. Similar arguments also make it appear unlikely that there would be an $ns \rightarrow (n-1)d$ transition at high compressions in the transition metals. This is contrary to the contention of Al'tshuler *et al.*[31] that a high pressure stiffening of the Hugoniots of several transition metals is caused by an $s \rightarrow d$ electronic transition.

The solid circles shown in Fig. 14 mark the Wigner-Seitz radii where the various rare-earth Hugoniots stiffen, i.e., the radii that correspond to the kinks in the (U_s, U_p) plots. Note that for La, Pr, Nd, Sm, Dy, Er, and probably Eu and Gd, this stiffening occurs only after the material has been compressed to a volume where the xenon cores overlap.

Figure 16 compares all the experimental Wigner-Seitz radii that correspond to the kinks in the (U_s, U_p) plots with the radii of several electronic shells at $P = 0$ bar. Note that for all elements, including the data of Al'shuler *et al.* for the nonrare earths, stiffening occurs after each material has been compressed to a volume where the noble-gas cores overlap.

This consistent response indicates that the stiffening of the Hugoniots is related to the onset of repulsive interaction between the noble-gas cores. Hence we assert that neither melting, solid-solid phase transition, nor electronic transitions are the cause of the kinks in the (U_s, U_p) plots.

The coefficients for the (U_s, U_p) straight-line relations are listed in Table V. The slopes of these lines represent the volume derivatives of the compressibilities for the materials. These data have been compared with similar results from Refs. 5 and 31. Except for Gd and Dy the slopes found for the initial line segments are in good agreement. Good agreement was also obtained for the slopes of the high-pressure segments for La, Ce, and Gd. The second slopes they report for the remaining elements tend to be somewhat steeper than ours. The Soviet data for the coordinates at the (U_s, U_p) kinks also are larger than ours. Their data was obtained at higher pressure, hence the extrapolations to the kinks are greater. The disagreement may also be related to differences in materials; their results do not include a statement concerning impurities.

Attempts to correlate the initial (U_s, U_p) slopes with crystal structures at low pressure (Table I) were not fruitful. The rare earths all have close-packed structures, and it appears that the initial slopes, roughly between 0.8 and 1.0, are more dependent on valence-electron structure than crystal array. There was no regular change of slope with atomic number. Ce, Eu, and Yb present anomalies in the resistance-pressure curves and are more compressible than the other rare earths. It may be recalled that these elements have empty half-filled and filled $4f$ shells.

Comparisons were also made with existing data for the actinide elements, thorium[41,42] and uranium.[43,44] The slopes for the (U_s, U_p) plots for these elements are single lines to pressures of 1.4 and 6.4 Mbar, respectively, and do not display the concave upwards kink. The magnitudes of the slopes, 1.27 and 1.50, are more consistent with the values for the second slopes of the lanthanides.

SUMMARY

(i) The (U_s, U_p) plots for all materials can be represented by straight lines. The plots for Y,

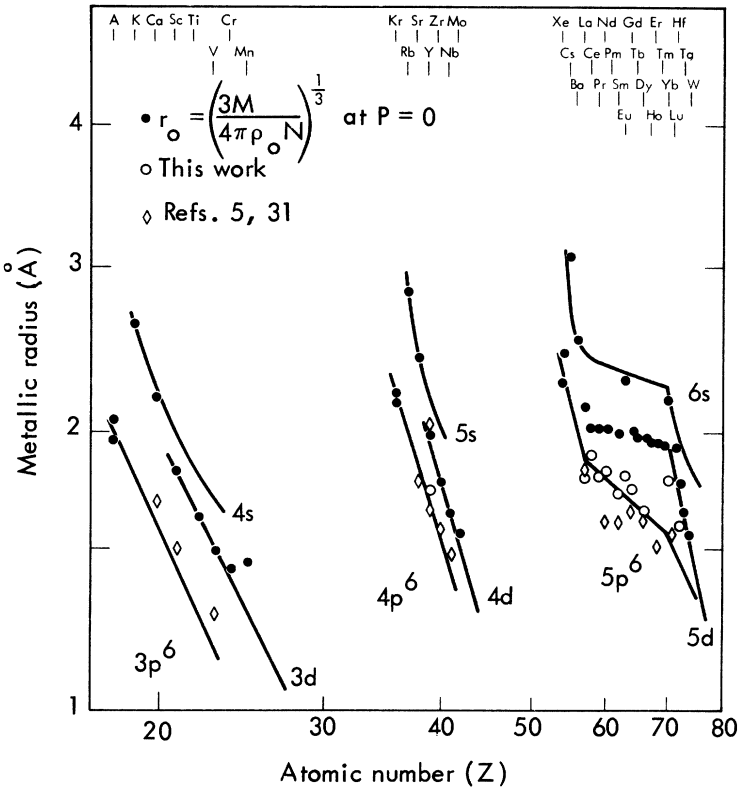

FIG. 16. Atomic radius vs atomic number for a number of elements at zero pressure and at pressures where the Hugoniots stiffen. The lines show the Z dependence obtained from Hartree-Fock free-atom solutions as normalized to the zero-pressure experimental data. Note that the radii obtained from the volumes where the Hugoniots stiffen for all elements, inclusing the non-rare-earths, plot very near the Hartree-Fock representations of the noble-gas shells (except Yb which has a polymorphic phase transition.)

La, Pr, Nd, Sm, Gd, Dy, and Hf consist of two line segments which are concave upwards and the intersection of these lines marks the region where the volume derivative of the compressibility is abruptly changed.

(ii) The plots for Ce do not resemble those of its neighbors.

(iii) It is shown that the kinks in the (U_s, U_p) plots do not appear to be manifestations of melting at high-pressure, solid-solid, or electronic phase transitions. Instead it is noted that the stiffening occurs after the materials, including non-rare-earths, are compressed to a volume where the noble-gas cores overlap. This is the first time such a core interaction has been identified in the compression of metals.

ACKNOWLEDGMENTS

We thank E. J. Nidick and W. Simpson for the tedious assembly of the experiments inside a dry box and L. J. Bacon and K. F. Humpherys for assistance at the high-explosive site. In the preparation of this report we have had the advantage of examining unpublished work on rare-earth metals by W. J. Carter.

*Work performed under the auspices of the U. S. Atomic Energy Commission.

[1]K. A. Gschneidner, Jr., *Rare Earth Alloys* (Van Nostrand, Princeton, N. J., 1961), or F. H. Spedding and A. H. Daane, *The Rare Earths* (Wiley, New York, 1961).

[2]Compendium Shockwave Data, edited by M. van Thiel, A. S. Kusubov, A. C. Mitchell, and V. W. Davis, Lawrence Livermore Laboratory Rept. UCRL-50108, 1966. (unpublished).

[3]E. B. Royce, Phys. Rev. **164**, 929 (1967).

[4]Preliminary reports on this work were presented in *Symposium on High Dynamic Pressures, Paris, France*, 1967 (Gordon and Breach, New York, 1968), p. 397, and at the Winter Meeting of the American Physical Society at Pasadena, December, 1967, [Bull. Am. Phys. Soc. **12**, 1128 (1967)].

[5]L. V. Al'tshuler, A. A. Bakanova, I. P. Dudoladov, Zh. Eksp. Teor. Fiz. Pis'ma Red. **3**, 483 (1966) [JETP Lett. **3**, 315 (1966)].

[6]P. W. Bridgman, Proc. Am. Acad. Arts Sci. **83**, 1 (1954).

[7]H. G. Drickamer, in *Solid State Physics*, edited by F. Seitz and D. Turnbull (Academic, New York, 1965), Vol. 17, pp. 89–111. A revised calibration, [H. G. Drickamer, Rev. Sci. Instrum. **41**, 1667 (1970)] indicates that the pressures corresponding to the various features in the resistance-pressure curves may be 10–15% high.

[8]H. D. Stromberg and D. R. Stephens, J. Phys. Chem. Solids **25**, 1015 (1964).

[9]A. Jayaraman and R. C. Sherwood, Phys. Rev. Lett. **12**, 22 (1964).

[10]A. Jayaraman and R. C. Sherwood, Phys. Rev. **134**, A691 (1964).

[11]G. J. Piermarini and C. E. Weir, Science **144**, 69 (1964).

[12]A. Jayaraman, *Physics of Solids at High Pressure*, edited by C. T. Tomsuka and R. M. Emrick (Academic, New York, 1965), p. 478.
[13]D. B. McWhan and A. L. Stevens, Phys. Rev. **139**, 682 (1965).
[14]E. Franceschi and G. L. Olcese, Phys. Rev. Lett. **22**, 1299 (1969).
[15]D. B. McWhan, Phys. Rev. B **1**, 2826 (1970).
[16]H. T. Hall, J. D. Baxhett, and L. Merrill, Science **139**, 111 (1963).
[17]D. R. Stephens, J. Phys. Chem. Solids **25**, 423 (1964).
[18]D. B. McWhan, T. M. Rice, and P. H. Schmidt, Phys. Rev. **177**, 103 (1969).
[19]A. W. Lawson and Ting-Yuan Tang, Phys. Rev. **76**, 301 (1949).
[20]J. Wittig, Phys. Rev. Lett. **21**, 1250 (1968).
[21]M. H. Rice, R. G. McQueen, and J. M. Walsh, in *Solid State Physics*, edited by F. Seitz and D. Turnbull (Academic, New York, 1958), Vol. 6, pp. 8 and 31.
[22]R. N. Keeler and E. B. Royce, in *Physics of High Energy Density* edited by P. Caldirola and H. Knoepfel (Academic, New York, 1971), pp. 51–150.
[23]R. G. McQueen, S. P. Marsh, J. W. Taylor, J. N. Fritz, and W. J. Carter, in *High Velocity Impact Phenomena*, edited by Ray Kinslow (Academic, New York, 1970), pp. 294ff.
[24]J. M. Walsh and R. H. Christian, Phys. Rev. **97**, 1544 (1955).
[25]R. H. Christian, Lawrence Livermore Laboratory, Rept. UCRL-4900 (1957) (unpublished).
[26]F. Rogers, Lawrence Livermore Laboratory, internal document STN No. 154 (1967) (unpublished). Readers outside the Laboratory who desire further information on LLL internal documents should address their inquiries to the Technical Information Department, Lawrence Livermore Laboratory, Livermore, California 94550.
[27]G. Henderson, B. Kuhn, and P. Knauss, Lawrence Livermore Laboratory, Internal Memoranda (1966 and 1967) (unpublished).
[28]J. F. Smith, C. E. Carlson, and F. H. Spedding, J. Met. 1212, (1957).
[29]P. W. Bridgman, Proc. Am. Acad. Arts Sci. **81**, 169 (1952) Proc. Am. Acad. Arts Sci. **83**, 1 (1954). See also F. P. Bundy and H. M. Strong, in *Solid State Physics*, edited by F. Seitz and D. Turnbull (Academic, New York, 1962), Vol. 13, p. 104.
[30]H. L. Brown, P. E. Armstrong, and C. P. Kempter, J. Less-Common Met. 11, 135 (1966).
[31]L. V. Al'tshuler, A. A. Bakanova, and I. P. Dudoladov, Zh. Eksp. Teor. Fiz. **53**, 1967 (1967) [Sov. Phys.-JETP **26**, 1115 (1968)].
[32]P. C. Soeurs and G. Jura, Science **140**, 481 (1963).
[33]H. T. Hall and L. Merrill, Inorg. Chem. **2**, 618 (1963).
[34]For a detailed description of the inclined-prism technique see: W. H. Gust and E. B. Royce, J. Appl. Phys. **42**, 1897 (1971).
[35]For a discussion of the two-wave shock structure see: D. Bancroft, E. Peterson, and S. Minshall, J. Appl. Phys. **27**, 291 (1956).
[36]R. G. McQueen, in *Metallurgy at High Pressure and High Temperature*, edited by K. A. Gschneider, Jr., M. T. Hepworth, and N. A. D. Parlee (Gordon and Breach, New York, 1964), p. 83.
[37]A. W. Lawson, Prog. Met. Phys. 6, (1956).
[38]Cited by R. Sternheimer, Phys. Rev. **78**, 3 (1949); Phys. Rev. **78**, 235 (1949).
[39]A. Jayaraman, R. C. Newton, and J. M. McDonough, Phys. Rev. **159**, 3 (1967); Phys. Rev. **159**, 527 (1967).
[40]A. A. Bakanova and I. P. Dudoladov, Zh. Eksp. Teor. Fiz. Pis'ma Red. **5**, 322 (1966) [JETP Lett. **5**, 265 (1967)].
[41]R. G. McQueen and S. P. Marsh, J. Appl. Phys. **31**, 1253 (1960).
[42]J. M. Walsh, M. H. Rice, R. G. McQueen, and F. L. Yarger, Phys. Rev. **108**, 169 (1957).
[43]I. C. Skidmore and E. Morris, *Thermodynamics of Nuclear Materials* (International Atomic Energy Agency, Vienna, 1962), pp. 173ff.
[44]J. W. Taylor, Los Alamos Scientific Laboratory, Rept. LADC 5626, 1963 (unpublished).